



# Elevated serum interleukin-8 is associated with enhanced intratumor neutrophils and reduced clinical benefit of immune-checkpoint inhibitors

Kurt A. Schalper<sup>1,11</sup>✉, Michael Carleton<sup>2,11</sup>, Ming Zhou<sup>3</sup>, Tian Chen<sup>3</sup>, Ye Feng<sup>3</sup>, Shu-Pang Huang<sup>3</sup>, Alice M. Walsh<sup>4</sup>, Vipul Baxi<sup>4</sup>, Dimple Pandya<sup>5</sup>, Timothy Baradet<sup>2</sup>, Darren Locke<sup>2</sup>, Qiuyan Wu<sup>5</sup>, Timothy P. Reilly<sup>5</sup>, Penny Phillips<sup>2</sup>, Venkata Nagineni<sup>1</sup>, Nicole Gianino<sup>1</sup>, Jianlei Gu<sup>6</sup>, Hongyu Zhao<sup>6</sup>, Jose Luis Perez-Gracia<sup>7,8</sup>, Miguel F. Sanmamed<sup>7,8,9,10,12</sup> and Ignacio Melero<sup>7,8,10,12</sup>✉

**Serum interleukin-8 (IL-8) levels and tumor neutrophil infiltration are associated with worse prognosis in advanced cancers. Here, using a large-scale retrospective analysis, we show that elevated baseline serum IL-8 levels are associated with poor outcome in patients (n=1,344) with advanced cancers treated with nivolumab and/or ipilimumab, everolimus or docetaxel in phase 3 clinical trials, revealing the importance of assessing serum IL-8 levels in identifying unfavorable tumor immunobiology and as an independent biomarker in patients receiving immune-checkpoint inhibitors.**

Immunostimulatory therapies targeting programmed cell death 1 (PD-1) and cytotoxic T-lymphocyte-associated protein 4 (CTLA-4) can produce prominent and lasting antitumor effects and are standard treatment for numerous malignancies<sup>1</sup>. However, clinical benefits vary across tumor types, and most patients progress despite treatment<sup>2,3</sup>. Early identification of patients who are insensitive to treatment could avoid ineffective therapies with potentially serious adverse effects. Diverse tumor and host factors associated with primary sensitivity and resistance to immune-checkpoint inhibitors include protein expression of programmed cell death 1 ligand 1 (PD-L1) in pretreatment tumor biopsy specimens, mismatch repair deficiency, microsatellite instability, number of somatic DNA mutations and/or tumor mutational burden (TMB), T-cell infiltration metrics (for example, the level of CD8<sup>+</sup> tumor-infiltrating lymphocytes or interferon- $\gamma$  (IFN $\gamma$ )-related mRNA signatures), gut microbiota composition and deleterious somatic variants (for example, *STK11* (also known as *LKB1*) and *PBRM1*)<sup>2,4</sup>. However, clinical implementation of these markers is challenging; to date, only PD-L1 detection in tumor or immune cells using immunohistochemistry (IHC), mismatch repair deficiency using IHC and microsatellite instability using polymerase chain reaction assays have received regulatory companion diagnostic approval for immune-checkpoint inhibitors<sup>2</sup>. Additional nonredundant and minimally invasive biomarkers are required.

C-X-C motif chemokine ligand 8 (CXCL8, also known as IL-8), the first chemokine to be discovered, is an angiogenic polypeptide

expressed in multiple cancers<sup>5</sup>. IL-8 potently regulates the chemotaxis of human neutrophils<sup>6,7</sup> and exerts direct protumorigenic effects, including the promotion of angiogenesis, tumor cell dedifferentiation (for example, epithelial–mesenchymal transition) and invasion and/or metastasis<sup>8</sup>. The impact of IL-8 chemoattractant activity for neutrophils and other T-cell-suppressive myeloid cells in cancer has been poorly understood until recently<sup>9</sup>. We reported early increases in serum IL-8 levels as a strong predictor of poor outcome in small retrospective cohorts of patients with advanced melanoma or non-small-cell lung cancer (NSCLC) who were treated with immune-checkpoint inhibitors, suggesting a link between IL-8 expression and ineffective antitumor immune reinvigoration<sup>10</sup>. Here we evaluated the effect of serum IL-8 levels on antitumor outcomes in patients with advanced cancer from four randomized phase 3 clinical trials. Associations between serum IL-8 levels and known immunotherapy biomarkers (for example, PD-L1 and TMB) and the tumor immune contexture were also investigated.

We measured baseline serum IL-8 levels in samples from 1,344 patients treated with nivolumab monotherapy or nivolumab plus ipilimumab in four phase 3 clinical studies: CheckMate 067 (melanoma); CheckMate 017 (squamous NSCLC (sqNSCLC)); CheckMate 057 (nonsquamous NSCLC (nsqNSCLC)); and CheckMate 025 (renal-cell carcinoma (RCC)). The objective response rate (ORR), progression-free survival (PFS) and overall survival (OS) of patients were assessed using receiver operator characteristic (ROC) curves. OS was used to derive 23 pg ml<sup>-1</sup> as a clinically relevant stratification cut-off (Extended Data Fig. 1). Patients who received immune-checkpoint inhibitors were independently stratified by this cut-off in each trial cohort. Baseline serum IL-8 levels of  $\geq 23$  pg ml<sup>-1</sup> were identified in 27.1–34.3% of patients and were associated with shorter OS across treatments and tumor types (Fig. 1a–f, Extended Data Figs. 2, 3). The most detrimental survival effect occurred in patients with melanoma treated with nivolumab plus ipilimumab in CheckMate 067: hazard ratio (HR) of 3.06 (95% confidence interval (CI), 2.13–4.41) between patients with high ( $\geq 23$  pg ml<sup>-1</sup>) and low ( $< 23$  pg ml<sup>-1</sup>) baseline serum IL-8

<sup>1</sup>Department of Pathology, Yale University School of Medicine, New Haven, CT, USA. <sup>2</sup>Department of Translational Medicine, Bristol-Myers Squibb, Princeton, NJ, USA. <sup>3</sup>Department of Global Biometric Sciences, Bristol-Myers Squibb, Princeton, NJ, USA. <sup>4</sup>Department of Translational Bioinformatics, Bristol-Myers Squibb, Princeton, NJ, USA. <sup>5</sup>Department of Research and Early Development, Bristol-Myers Squibb, Princeton, NJ, USA. <sup>6</sup>Department of Biostatistics, School of Public Health, Yale University, New Haven, CT, USA. <sup>7</sup>Oncology Department, Clinica Universidad de Navarra, Pamplona, Spain. <sup>8</sup>Centro de Investigación Biomédica en Red de Cáncer (CIBERONC), Madrid, Spain. <sup>9</sup>Department of Immunobiology, Yale University School of Medicine, New Haven, CT, USA. <sup>10</sup>Department of Immunology and Immunotherapy, Centro de Investigación Médica Aplicada (CIMA), Universidad de Navarra, Pamplona, Spain. <sup>11</sup>These authors contributed equally: Kurt A. Schalper, Michael Carleton. <sup>12</sup>These authors jointly supervised this work: Miguel F. Sanmamed, Ignacio Melero. ✉e-mail: [kurt.schalper@yale.edu](mailto:kurt.schalper@yale.edu); [imelero@unav.es](mailto:imelero@unav.es)

levels. An HR of 1.84 (95% CI, 1.19–2.83) was detected in patients with advanced sqNSCLC from CheckMate 017. Similarly, a lower ORR was observed in patients with high ( $\geq 23$  pg ml<sup>-1</sup>) versus low ( $< 23$  pg ml<sup>-1</sup>) baseline serum IL-8 levels across most trials and treatment arms investigated (Extended Data Fig. 4, Supplementary Data 1). The association between elevated baseline serum IL-8 level and reduced survival was also observed in non-immunotherapy trial arms, including patients with RCC treated with single-agent everolimus (CheckMate 025) and patients with nsqNSCLC treated with docetaxel (CheckMate 057; Extended Data Fig. 3). The interaction term analysis between the outcome effect of IL-8 levels and immune-checkpoint inhibitors versus non-immunotherapies was not statistically significant, supporting the idea that elevated baseline serum IL-8 levels are associated with negative prognosis.

The proportion of patients with elevated baseline serum IL-8 levels was similar between patients with positive and negative PD-L1 expression (1% cut-off) (Extended Data Fig. 5). The correlation between PD-L1 expression level and baseline serum IL-8 level was low across tumor types (Spearman's correlation coefficient ( $\rho$ ),  $-0.069$ – $0.107$ ;  $\rho$  for all studies combined,  $-0.028$ ) (Fig. 1g–j). Therefore, the IL-8-mediated effect on survival is independent of PD-L1 IHC positivity.

To address the possible association between tumor IL-8 levels and TMB, we studied *CXCL8* mRNA levels and somatic mutation numbers in select tumor cohorts from The Cancer Genome Atlas (TCGA) dataset. The low correlation between *CXCL8* transcript expression and TMB across tumor types (Spearman's  $\rho$ ,  $0.0073$ – $0.1458$ ) (Extended Data Fig. 6) supports a limited association.

To evaluate the relationship between IL-8 and inflammatory responses, we studied the association between serum IL-8 levels, tumor expression of key immune transcripts, and selected circulating immune-cell populations. Circulating IL-8 level was positively correlated with tumor *CXCL8* gene expression and blood neutrophil and monocyte counts (Fig. 2a). Increased tumor IL-8 level was negatively associated with tumor IFN $\gamma$ - and T-cell infiltration-related transcript signatures. A positive association between local IL-8 protein expression in the tumor and increased tumor infiltration by myeloperoxidase (MPO)<sup>+</sup> and/or CD15<sup>+</sup> monocytes and neutrophils was identified using multiplexed quantitative and spatially resolved immunofluorescence analyses of retrospective tumor specimens from NSCLC (Fig. 2b–d), melanoma (Fig. 2e–g) and RCC (Fig. 2h–j). These data provide evidence of IL-8 production in tumor cells, support an adaptive immune suppressive effect of IL-8 and suggest a strong association between tumor-derived IL-8 and tolerogenic myeloid-cell infiltration in the tumor microenvironment.

These results validate and expand the strong prognostic influence of IL-8 in multiple tumor types across treatment settings. Our analyses demonstrate an independent survival effect of serum

IL-8 levels across four tumor types from randomized clinical trial data and show a consistent association with tumor-infiltrating neutrophils and/or monocytes. We also propose a clinically meaningful cut-off level of 23 pg ml<sup>-1</sup>. Serum IL-8 level is a simple quantitative parameter that can be easily measured in conventional blood specimens in clinical settings.

IL-8 is a powerful chemoattractant for neutrophils and other potentially immune-suppressive myeloid leukocytes<sup>9</sup>. We observed that IL-8 expression correlated with neutrophil and monocyte abundance in IL-8-producing tumors, consistent with evidence from gene signatures indicating that polymorphonuclear leukocyte proliferation, or increased circulating neutrophils over lymphocytes, is associated with poor prognosis in patients with cancer<sup>11,12</sup>. High *CXCL8* mRNA expression negatively correlated with T-cell markers and IFN $\gamma$ -dependent gene signatures in the tumor microenvironment. These associations suggest that mechanisms of T-cell exclusion and immunosuppression involve myeloid-derived suppressor cells, as observed in mice<sup>13,14</sup>. Baseline serum IL-8 levels likely reflect tumor IL-8 production and a unique, unfavorable tumor microenvironment characterized by prominent myeloid-cell infiltration, including neutrophils and monocytes, and limited adaptive T-cell responses. Distinct from known immune-checkpoint inhibitor-associated biomarkers, IL-8 could be part of and complement robust multiparameter immunotherapy biomarker signatures. Ongoing studies are assessing differences in IL-8 levels and dynamics across diseases and clinical settings.

Elevated baseline serum IL-8 levels were associated with adverse outcomes in melanoma, sqNSCLC, nsqNSCLC and RCC. To date, biomarkers such as microsatellite instability and TMB have not shown a survival effect or predictive value in RCC. Assessment of serum IL-8 levels could expand the biomarker arsenal for optimal immune-checkpoint inhibitor use in tumors that currently lack clinically useful biomarkers. Analysis of the potential mechanistic role of IL-8 with respect to immune-checkpoint inhibitor response (by neutralizing IL-8 or inhibiting IL-8 receptors) is needed.

We determined that 23 pg ml<sup>-1</sup> is a clinically relevant stratification cut-off using pooled analyses. Despite differences in median survival across individual studies, the 23 pg ml<sup>-1</sup> cut-off produces a comparable Youden's index to its maximum value for nivolumab-containing arms in both individual and pooled studies, demonstrating that this cut-off could be applied to melanoma, sqNSCLC, nsqNSCLC and RCC. The numerical values of IL-8 measurements may vary slightly depending on the analytical method used.

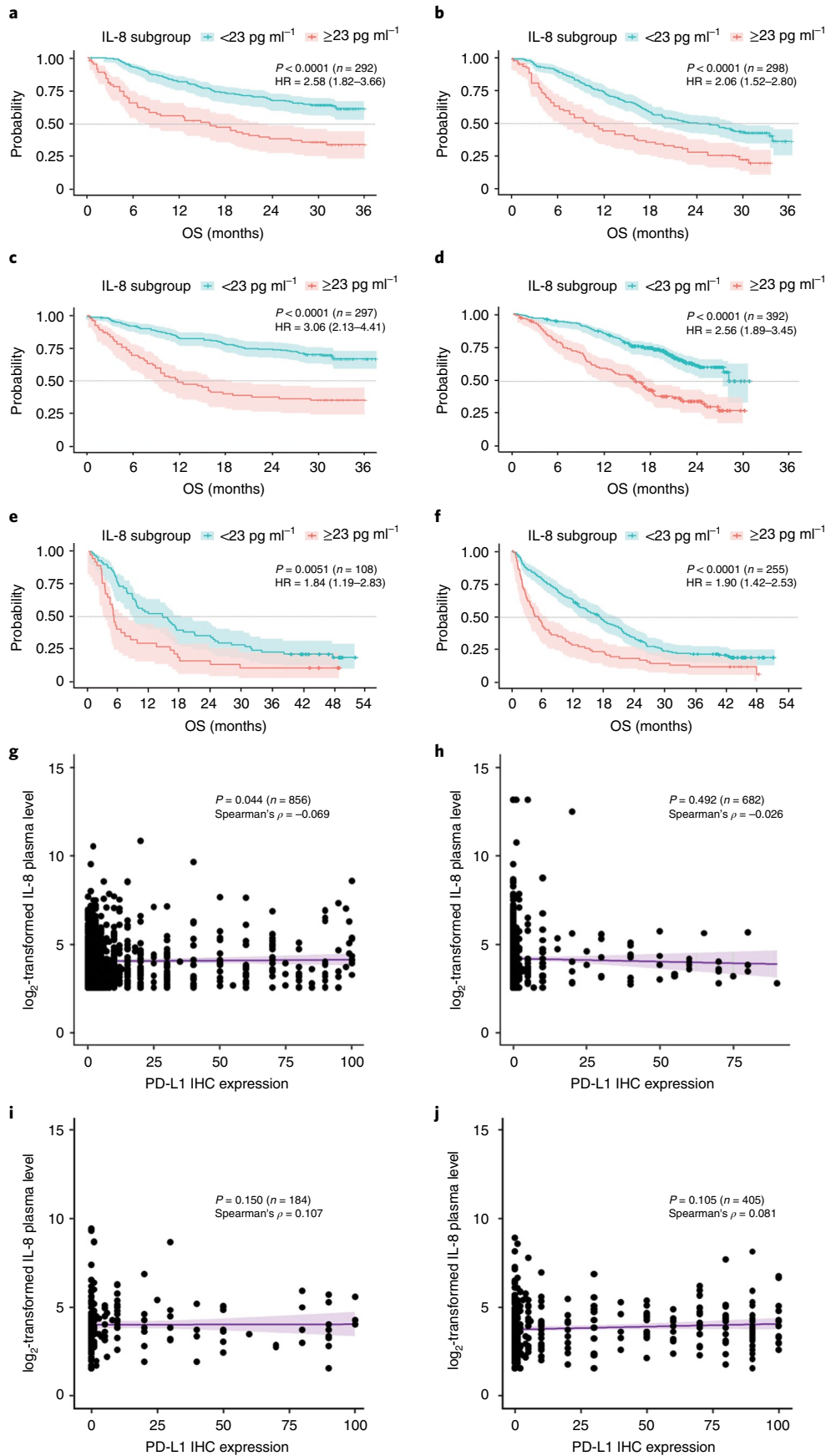
Our results show that elevated IL-8 levels are associated with adverse tumor features and can be used as a negative prognostic marker in patients treated with different therapies including immune-checkpoint inhibitors. We cannot exclude a role for IL-8 in predicting resistance to specific anticancer immunotherapies in

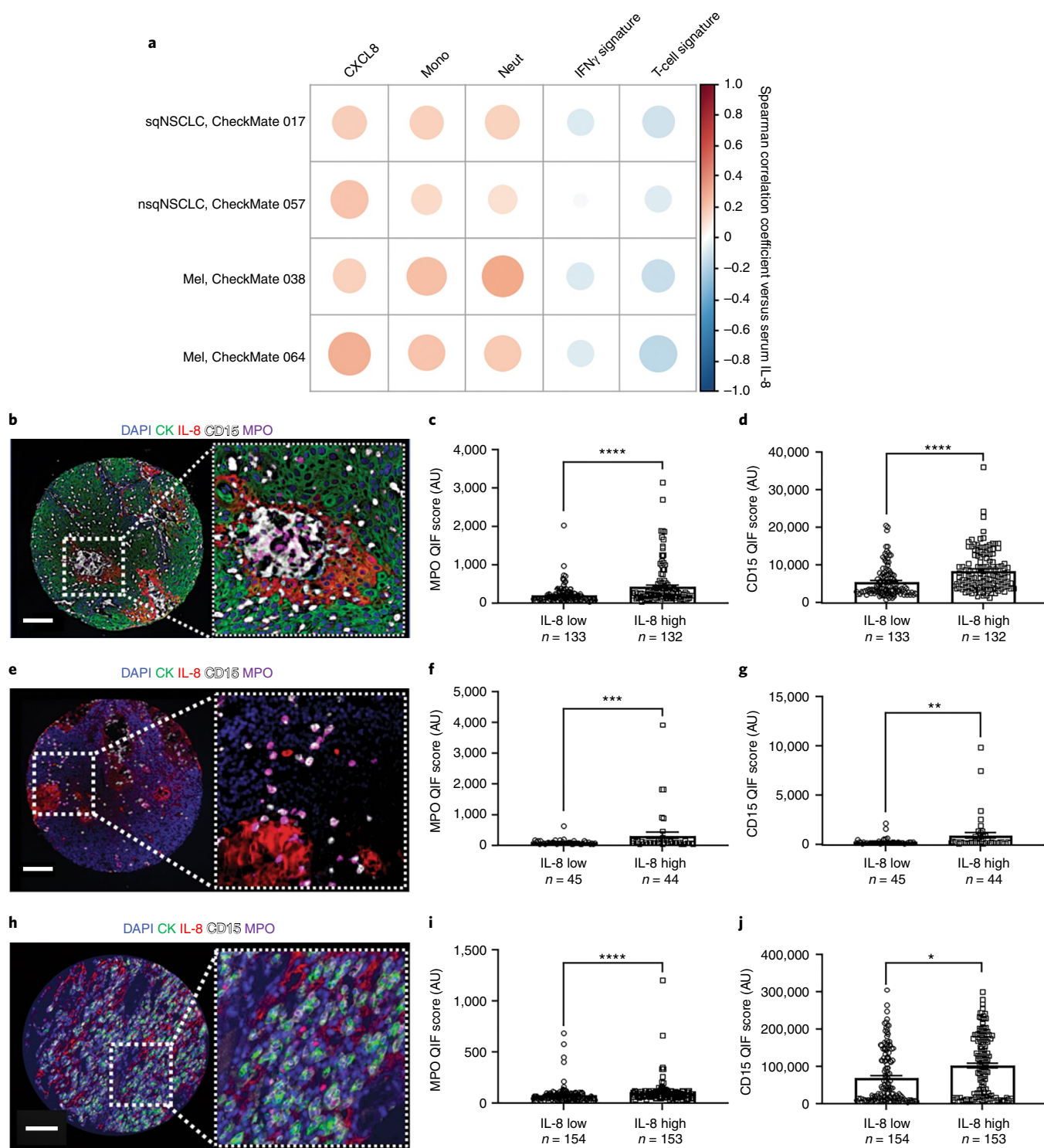
### Fig. 1 | Association between baseline serum IL-8 level and survival and baseline PD-L1 level in patients treated with immune-checkpoint inhibitors.

**a–f**, Exploratory Kaplan–Meier analysis of the OS probability (with 95% confidence intervals) in patients with melanoma (CheckMate 067) (**a–c**; **a**, nivolumab; **b**, ipilimumab; **c**, nivolumab and ipilimumab), RCC (CheckMate 025) (**d**; nivolumab), sqNSCLC (CheckMate 017) (**e**; nivolumab) and nsqNSCLC (CheckMate 057) (**f**; nivolumab) treated with PD-1 and CTLA-4 blockers in four prospective phase 3 clinical trials. Patients were stratified using a serum IL-8 level of 23 pg ml<sup>-1</sup>. The specific study, two-sided log-rank test *P* values for the survival analysis, the number of independent patients with available IL-8 and OS data (*n*) and the OS HR (based on Cox proportional hazard models) between IL-8 subgroups ( $\geq 23$  pg ml<sup>-1</sup> versus  $< 23$  pg ml<sup>-1</sup>) are shown. The dotted lines indicate the 50% probability of OS. **g–j**, The association between the tumor PD-L1 level by IHC analysis and the log<sub>2</sub>-transformed serum IL-8 level in patients with melanoma (CheckMate 067, *n* = 856; Spearman's correlation coefficient,  $\rho$  =  $-0.069$ ) (**g**), RCC (CheckMate 025, *n* = 682;  $\rho$  =  $-0.026$ ) (**h**), sqNSCLC (CheckMate 017, *n* = 184;  $\rho$  =  $0.107$ ) (**i**) and nsqNSCLC (CheckMate 057, *n* = 405;  $\rho$  =  $0.081$ ) (**j**). *P* values for the two-sided Spearman's test (based on *t*-distribution approximation with *n* – 2 degrees of freedom) of the association between tumor PD-L1 level and the log<sub>2</sub>-transformed serum IL-8 level, the number of independent patients (*n*) with paired PD-L1 and serum IL-8 data for each study and Spearman's correlation coefficients ( $\rho$ ) are shown. PD-L1 levels were determined using IHC with the DAKO PD-L1 IHC 28-8 pharmDx assay (Agilent), read by a pathologist and expressed as the percentage of positive tumor cells. Baseline serum IL-8 levels were determined by immunoassay and expressed as log<sub>2</sub>-transformed values of the protein concentration. Each dot indicates an individual patient; the purple line shows the linear regression line (with 95% confidence intervals). There are no multiplicity adjustments made for all statistical analyses.

tumor types or treatment settings not included in our study. The unfavorable outcome associated with elevated IL-8 is likely mediated by its negative immunomodulatory effect. Other anticancer

treatments, such as cytotoxic chemotherapy and targeted agents, have also been shown to induce immune stimulation, and an intact adaptive immune response is one of the factors required to mediate





their therapeutic effect<sup>15</sup>. Although the contribution of the prognostic and a possible negative predictive effect of IL-8 cannot be fully resolved due to the retrospective design and statistical considerations of this study, patients with high pretreatment IL-8 levels are less likely to benefit from immune-checkpoint inhibitors.

In addition to its possible role as a prognostic biomarker, IL-8 is being considered as a candidate therapeutic target<sup>16</sup>. IL-8 reportedly exerts proangiogenic functions that may underlie escape from vascular endothelial growth factor–vascular endothelial growth factor receptor inhibitors and mediates direct effects on malignancy-sustaining cancer stem cells and the epithelial–mesenchymal

transition of tumor cells<sup>5,17</sup>. Agents targeting IL-8 or IL-8 receptors are in clinical development<sup>16</sup>; selective inhibitors of the IL-8 receptor CXCR2 are in late preclinical or clinical development in combination with immune-checkpoint inhibitors (ClinicalTrials.gov identifiers [NCT02499328](#), [NCT03473925](#) and [NCT03161431](#)). Anti-IL-8 therapies could complement immune-checkpoint inhibitors by suppressing immuno-oncology-resistance pathways. A fully human monoclonal anti-IL-8 antibody (BMS-986253) has been shown to be safe in patients with advanced cancers<sup>16</sup>. Ongoing studies are evaluating the safety and efficacy of BMS-986253 in combination with nivolumab ([NCT03400332](#)).

**Fig. 2 | Association between IL-8 levels and monocytes and neutrophils in human malignancies.** **a**, Association between serum IL-8 levels and tumor mRNA expression of *CXCL8*, peripheral monocyte counts (Mono), blood neutrophil counts (Neut), IFN $\gamma$ -related gene signature<sup>18</sup> and the T-cell-related mRNA signature<sup>19</sup> in patients with sqNSCLC (CheckMate 017,  $n=113$ ), nsqNSCLC (CheckMate 057,  $n=248$ ) or melanoma (Mel; CheckMate 038,  $n=142$ ; CheckMate 064,  $n=127$ ). The color intensity of the circles indicates the Spearman's correlation coefficient of the association. Darker red, larger dots represent a greater correlation between serum IL-8 level and the indicated factor; darker blue, larger dots represent a greater negative correlation between serum IL-8 level and the indicated factor. **b**, Representative fluorescence image of 265 samples from one tumor showing the simultaneous detection of 4',6-diamidino-2-phenylindole (DAPI; blue), cytokeratin (CK; green), IL-8 (red), CD15 (white) and MPO (magenta) in human NSCLC. **c,d**, Association between tumor IL-8 protein and MPO (**c**) or CD15 (**d**) levels in NSCLC (independent biological samples). **e**, Representative fluorescence image of 99 samples from one tumor showing the simultaneous detection of DAPI (blue), cytokeratin (green), IL-8 (red), CD15 (white) and MPO (magenta) in human melanoma. **f,g**, Association between tumor IL-8 protein and MPO (**f**) or CD15 (**g**) levels in melanoma (independent biological samples). **h**, Representative fluorescence image of 307 samples from one tumor showing the simultaneous detection of DAPI (blue), cytokeratin (green), IL-8 (red), CD15 (white) and MPO (magenta) in human RCC. **i,j**, Association between tumor IL-8 protein and MPO (**i**) or CD15 (**j**) levels in RCC (independent biological samples). Patients were stratified using the median score as the cut-off. The number of patients ( $n$ ) is indicated.  $P$  values for the 2-sided Mann-Whitney  $U$ -test: \* $P < 0.0001$ ; \*\*\* $P = 0.0195$ ; \*\* $P = 0.0129$ ; \* $P = 0.0003$ . Error bars indicate standard of error of the mean. Scale bars, 100  $\mu\text{m}$ . AU, arbitrary units; QIF, quantitative immunofluorescence.

### Online content

Any methods, additional references, Nature Research reporting summaries, source data, extended data, supplementary information, acknowledgements, peer review information; details of author contributions and competing interests; and statements of data and code availability are available at <https://doi.org/10.1038/s41591-020-0856-x>.

Received: 27 July 2019; Accepted: 25 March 2020;  
Published online: 11 May 2020

### References

- Ribas, A. & Wolchok, J. D. Cancer immunotherapy using checkpoint blockade. *Science* **359**, 1350–1355 (2018).
- Havel, J. J., Chowell, D. & Chan, T. A. The evolving landscape of biomarkers for checkpoint inhibitor immunotherapy. *Nat. Rev. Cancer* **19**, 133–150 (2019).
- O'Donnell, J. S., Teng, M. W. L. & Smyth, M. J. Cancer immunoeediting and resistance to T cell-based immunotherapy. *Nat. Rev. Clin. Oncol.* **16**, 151–167 (2019).
- Schalper, K. A., Kaftan, E. & Herbst, R. S. Predictive biomarkers for PD-1 axis therapies: the hidden treasure or a call for research. *Clin. Cancer Res.* **22**, 2102–2104 (2016).
- Moore, B. B. et al. Distinct CXC chemokines mediate tumorigenicity of prostate cancer cells. *Am. J. Pathol.* **154**, 1503–1512 (1999).
- Baggiolini, M. CXCL8 — the first chemokine. *Front. Immunol.* **6**, 285 (2015).
- Baggiolini, M., Walz, A. & Kunkel, S. L. Neutrophil-activating peptide-1/interleukin 8, a novel cytokine that activates neutrophils. *J. Clin. Invest.* **84**, 1045–1049 (1989).
- David, J. M., Dominguez, C., Hamilton, D. H. & Palena, C. The IL-8/IL-8R axis: a double agent in tumor immune resistance. *Vaccines* **4**, 22 (2016).
- Alfaro, C. et al. Tumor-produced interleukin-8 attracts human myeloid-derived suppressor cells and elicits extrusion of neutrophil extracellular traps (NETs). *Clin. Cancer Res.* **22**, 3924–3936 (2016).
- Sanmamed, M. F. et al. Changes in serum interleukin-8 (IL-8) levels reflect and predict response to anti-PD-1 treatment in melanoma and non-small-cell lung cancer patients. *Ann. Oncol.* **28**, 1988–1995 (2017).
- Templeton, A. J. et al. Prognostic role of neutrophil-to-lymphocyte ratio in solid tumors: a systematic review and meta-analysis. *J. Natl Cancer Inst.* **106**, dju124 (2014).
- Coffelt, S. B., Wellenstein, M. D. & de Visser, K. E. Neutrophils in cancer: neutral no more. *Nat. Rev. Cancer* **16**, 431–446 (2016).
- Kapanadze, T. et al. Regulation of accumulation and function of myeloid derived suppressor cells in different murine models of hepatocellular carcinoma. *J. Hepatol.* **59**, 1007–1013 (2013).
- Gabrilovich, D. I., Ostrand-Rosenberg, S. & Bronte, V. Coordinated regulation of myeloid cells by tumours. *Nat. Rev. Immunol.* **12**, 253–268 (2012).
- Wargo, J. A., Reuben, A., Cooper, Z. A., Oh, K. S. & Sullivan, R. J. Immune effects of chemotherapy, radiation, and targeted therapy and opportunities for combination with immunotherapy. *Semin. Oncol.* **42**, 601–616 (2015).
- Bilusic, M. et al. Phase I trial of HuMax-IL8 (BMS-986253), an anti-IL-8 monoclonal antibody, in patients with metastatic or unresectable solid tumors. *J. Immunother. Cancer* **7**, 240 (2019).
- Conroy, S., Kruyt, F. A. E., Wagemakers, M., Bhat, K. P. L. & den Dunnen, W. F. A. IL-8 associates with a pro-angiogenic and mesenchymal subtype in glioblastoma. *Oncotarget* **9**, 15721–15731 (2018).
- Ayers, M. et al. IFN- $\gamma$ -related mRNA profile predicts clinical response to PD-1 blockade. *J. Clin. Invest.* **127**, 2930–2940 (2017).
- Siemers, N. O. et al. Genome-wide association analysis identifies genetic correlates of immune infiltrates in solid tumors. *PLoS ONE* **12**, e0179726 (2017).

**Publisher's note** Springer Nature remains neutral with regard to jurisdictional claims in published maps and institutional affiliations.

© The Author(s), under exclusive licence to Springer Nature America, Inc. 2020

## Methods

**Analyzed studies.** Exploration of the association between serum IL-8 level and survival. Patients ( $n = 1,344$ ) treated with nivolumab or nivolumab and ipilimumab (immune-checkpoint inhibitors) in four phase 3 clinical trials (CheckMate 067, melanoma<sup>30</sup>; CheckMate 017, sqNSCLC<sup>21</sup>; CheckMate 057, nsqNSCLC<sup>22</sup>; CheckMate 025, RCC<sup>23</sup>) (Extended Data Fig. 8) were included for analyses. Serum IL-8 levels were measured at baseline using the human multianalyte profile (MAP) immunoassay platform (Myriad RBM)<sup>34</sup> (Fig. 1, Supplementary Data 1, Extended Data Fig. 7). The total number of cases for exploration of the association between serum IL-8 level and survival—including the ipilimumab arm of CheckMate 067 and non-immune-checkpoint inhibitor arms of CheckMate 057 and CheckMate 025—was 2,243 patients.

**Gene-expression analyses.** The association between serum IL-8 levels and tumor *CXCL8* mRNA expression at baseline was analyzed in samples for which serum IL-8 levels, gene expression and complete blood count data were available. The following numbers of unique cases were analyzed: CheckMate 017,  $n = 113$ ; CheckMate 038 (refs. 25,26),  $n = 142$  and  $n = 248$ , respectively; CheckMate 064 (ref. 27),  $n = 127$ .

**Outcome measures.** The primary objective of this exploratory analysis was to assess the association between baseline serum IL-8 levels and antitumor activity; efficacy measures included ORR, PFS and OS.

**Statistical methods.** To determine a clinically relevant cut-off for baseline serum IL-8 levels, we conducted time-dependent ROC curve analyses<sup>28</sup> on OS (12 months), ORR and PFS (6 months) for all patients treated with nivolumab-containing therapies combined across the four studies (Extended Data Fig. 1). Because the OS ROC curve produces the highest area under the curve (AUC = 0.685) among OS, ORR and PFS, the Youden's index (sensitivity + specificity - 1) for the OS ROC curve was the only metric considered to select the cut-off of 23 pg ml<sup>-1</sup> (Supplementary Data 1). OS ROC analyses were also conducted to assess the cut-off of 23 pg ml<sup>-1</sup> for the immune-checkpoint inhibitor arms of individual studies (Extended Data Fig. 7). We used Kaplan-Meier analyses to assess OS stratified by serum IL-8 levels (cut-off, 23 pg ml<sup>-1</sup>) and compared the OS between IL-8 subgroups ( $\geq 23$  pg ml<sup>-1</sup> versus  $< 23$  pg ml<sup>-1</sup>) using two-sided log-rank tests for each study (Fig. 1a-f). Kaplan-Meier curves of OS stratified by serum IL-8 quartiles for nivolumab-containing therapies combined across the four studies (Extended Data Fig. 9) were also obtained. In addition, we evaluated the Spearman's correlation coefficient between PD-L1 IHC scores (Fig. 1g-j), determined using the DAKO PD-L1 IHC 28-8 pharmDx assay (Agilent) and expressed as the percentage of positive tumor cells and (log<sub>2</sub>-transformed) serum IL-8 levels. The Spearman's correlation coefficient was then tested using a two-sided Spearman's test (based on *t*-distribution approximation with  $n - 2$  degrees of freedom, where  $n$  is the number of independent patients with paired PD-L1 and IL-8 data) for each study. To assess the association between serum IL-8 level and OS, accounting for tumor PD-L1 expression, we also conducted a Cox proportional hazards model of OS, adjusting for baseline serum IL-8 level, PD-L1 IHC score and baseline tumor burden estimated as the sum of target lesion size.

**IL-8 expression and TMB in TCGA.** We collected gene-expression and somatic-variant data for 1,424 samples over four cancer types, including sqNSCLC, nsqNSCLC, RCC and melanoma<sup>29</sup>. We used the somatic variants as determined by and passed through the filtering by TCGA and gene-expression level-3 data represented as fragments per kilobase per million mapped reads (FPKM). TMB was defined by whole-exome sequencing, as previously described<sup>30</sup>, including all base substitutions and small insertions or deletions in the coding region of targeted genes. To calculate the TMB per megabase, the total number of somatic mutations counted was divided by the total size of the exonic region of the human genome.

$$TMB = n \times \frac{1,000,000}{33,763,157}$$

where  $n$  is the raw somatic variant count as determined by TCGA. We used 33 Mb as the estimate of the size of the exome. To test for the correlation between *CXCL8* mRNA expression levels and TMB, we transformed the FPKM value of IL-8 and total mutational counts to a log<sub>10</sub> scale, and the Spearman's correlation coefficients were calculated (Extended Data Fig. 6).

**Gene-expression analyses.** Gene-expression data (HTG EdgeSeq Oncology Biomarker Panel; HTG Molecular Diagnostics) were generated from archival biopsy specimens or biopsy specimens obtained at screening before baseline serum sample acquisition. Monocyte and neutrophil counts were generated using standard complete blood counts. Correlations and figures were generated with R v.3.5.1 and corrplot package v.0.84. Gene-expression signature scores were calculated based on a list of genes using the median *z*-scores of the normalized values of all genes in a given list (for example, IFN $\gamma$ -related gene signature<sup>18</sup> or T-cell gene signature<sup>19</sup>) for each sample. The *z*-scores of normalized gene expression values for *CXCL8* were used for correlative analyses. Spearman's correlation coefficients between baseline serum IL-8 levels and other baseline

biomarker measurements were calculated as indicated (Fig. 2a; *CXCL8* data and gene-expression scores are included in Supplementary Data 1).

**Retrospective patient cohorts and tissue microarrays.** We included retrospectively collected formalin-fixed, paraffin-embedded tumor samples from 265 primary NSCLCs, 99 primary melanomas and 307 RCCs collected at Yale University/Yale New Haven Hospital, provided in tissue microarray (TMA) format (Fig. 2b,e,h). As previously described<sup>31</sup>, TMAs were constructed by selecting areas containing viable tumor cells and stromal elements without enriching for specific tumor regions, tissue structures or immune-related features on preparations stained with hematoxylin and eosin (as assessed by a pathologist). All tissue and clinical QIF information were used after approval from the Yale Human Investigation Committee (protocols 9505008219 and 1608018220), which approved the patient consent forms or waivers of consent.

**Multiplexed immunofluorescence analysis.** Using previously validated and standardized multiplexed immunofluorescence protocols and TMA sections<sup>32,33</sup>, we simultaneously measured the levels of 4',6-diamidino-2-phenylindole (DAPI), pan-cytokeratin clone AE1/AE3 (1:100 dilution; 53-9003-82, eBioscience), IL-8 clone 807 (1:5,000 dilution; ab18672, Abcam), myeloperoxidase clone E1E71 (1:1,000 dilution; 14569, Cell Signaling Technology) and CD15 clone MC480 (1:2,000 dilution; 4744S, Cell Signaling Technology) (Fig. 2b-j, source data are provided in Supplementary Data 1). In brief, TMA sections were deparaffinized, and antigens were recovered with EDTA (1 mmol l<sup>-1</sup>, pH 8; Sigma-Aldrich) and boiling for 20 min at 97 °C (Lab Vision PT module; Thermo Fisher Scientific)<sup>31</sup>. Endogenous peroxidase was inactivated by the addition of a DAKO endoperoxidase inhibitor solution for 10 min, and the slides were incubated with a blocking solution containing 0.3% bovine serum albumin in 0.05% Tween-20 and Tris-buffered saline for 30 min. Primary antibody dilution and incubation were carried out simultaneously using the optimal dilution for each assay. Isotype-specific horseradish peroxidase-conjugated antibodies and tyramide-based amplification systems (PerkinElmer) were used for signal detection. The secondary antibodies and fluorescent reagents used were anti-rabbit EnVision (K4003, DAKO) with fluorescein-tyramide (PerkinElmer), anti-mouse IgG2a antibody (Abcam) with Cy3 plus (PerkinElmer), goat anti-rabbit (Abcam) with biotinylated tyramide/streptavidin-Alexa750 conjugate (PerkinElmer) and anti-mouse Envision (K40001; DAKO) with Cy5-tyramide (PerkinElmer). Residual horseradish peroxidase activity between sequential detection protocols was eliminated by incubating the slides twice with a solution containing benzoic hydrazide (100 mmol l<sup>-1</sup>) and hydrogen peroxide (50 mmol l<sup>-1</sup>) in phosphate-buffered saline. The fluorescence signal was measured in marker-selected tissue compartments using the automated AQUA platform (Navigate BioPharma).

**Reporting Summary.** Further information on research design is available in the Nature Research Reporting Summary linked to this article.

## Data availability

K.A.S.'s laboratory designed, conducted, analyzed and interpreted the data presented in Fig. 2b-j and Extended Data Fig. 6 (Yale Human Investigation Committee protocols 9505008219 and 1608018220). Bristol-Myers Squibb funded the studies CheckMate 067 (NCT01844505), CheckMate 017 (NCT01642004), CheckMate 057 (NCT01673867), CheckMate 025 (NCT01668784), CheckMate 038 (NCT01621490) and CheckMate 064 (NCT01783938) and participated in the design, conduct, analyses, and interpretation of these studies and related data (Figs. 1, 2a, Extended Data Figs. 1-3, 5, 7-9). Source data for Figs. 1, 2 and Extended Data Fig. 4 are provided in Supplementary Data 1. Bristol-Myers Squibb's policy on data sharing may be found at <https://www.bms.com/researchers-and-partners/independent-research/data-sharing-request-process.html>.

## References

- Larkin, J. et al. Combined nivolumab and ipilimumab or monotherapy in untreated melanoma. *N. Engl. J. Med.* **373**, 23-34 (2015).
- Brahmer, J. et al. Nivolumab versus docetaxel in advanced squamous-cell non-small-cell lung cancer. *N. Engl. J. Med.* **373**, 123-135 (2015).
- Borghaei, H. et al. Nivolumab versus docetaxel in advanced nonsquamous non-small-cell lung cancer. *N. Engl. J. Med.* **373**, 1627-1639 (2015).
- Motzer, R. J. et al. Nivolumab versus everolimus in advanced renal-cell carcinoma. *N. Engl. J. Med.* **373**, 1803-1813 (2015).
- Carleton, M. et al. Serum interleukin 8 (IL-8) may serve as a biomarker of response to immuno-oncology (I-O) therapy. *J. Clin. Oncol.* **36**, 3025 (2018).
- Ribas, A. et al. Immunomodulatory effects of nivolumab and ipilimumab in combination or nivolumab monotherapy in advanced melanoma patients: CheckMate 038. *Cancer Res.* **77**, CT073 (2017).
- Riaz, N. et al. Tumor and microenvironment evolution during immunotherapy with nivolumab. *Cell* **171**, 934-949 (2017).
- Weber, J. S. et al. Sequential administration of nivolumab and ipilimumab with a planned switch in patients with advanced melanoma (CheckMate 064): an open-label, randomised, phase 2 trial. *Lancet Oncol.* **17**, 943-955 (2016).

28. Heagerty, P. J., Lumley, T. & Pepe, M. S. Time-dependent ROC curves for censored survival data and a diagnostic marker. *Biometrics*. **56**, 337–344 (2000).
29. The Cancer Genome Atlas Research Network et al. The Cancer Genome Atlas Pan-Cancer analysis project. *Nat. Genet.* **45**, 1113–1120 (2013).
30. Chalmers, Z. R. et al. Analysis of 100,000 human cancer genomes reveals the landscape of tumor mutational burden. *Genome Med.* **9**, 34 (2017).
31. Villarreal-Espindola, F. et al. Spatially resolved and quantitative analysis of VISTA/PD-1H as a novel immunotherapy target in human non-small cell lung cancer. *Clin. Cancer Res.* **24**, 1562–1573 (2018).
32. Datar, I. et al. Expression analysis and significance of PD-1, LAG-3, and TIM-3 in human non-small cell lung cancer using spatially resolved and multiparametric single-cell analysis. *Clin. Cancer Res.* **25**, 4663–4673 (2019).
33. Schalper, K. A. et al. Objective measurement and clinical significance of TILs in non-small cell lung cancer. *J. Natl Cancer Inst.* **107**, dju435 (2015).

## Acknowledgements

We thank the patients and their families who made this study possible and the clinical study teams who participated in this study; DAKO for collaborative development of the PD-L1 IHC 28-8 pharmDx assay; Bristol-Myers Squibb and ONO Pharmaceutical Company Ltd. This study was supported by Bristol-Myers Squibb, Yale SPOR in Lung Cancer (P50CA196530), Department of Defense–Lung Cancer Research Program (W81XWH-16-1-0160), Yale Cancer Center Support Grant (P30CA016359), Stand Up To Cancer–American Cancer Society Lung Cancer Dream Team Translational Research Grant (SU2C-AACR-DT1715 and SU2C-AACR-DT22-17) and a grant from the Mark Foundation (19-029-MIA). I.M. is funded by MINECO SAF2017-83267-C2-1-R (AEI/FEDER, UE; I.M.), European Union's Horizon 2020 research and innovation program (635122, PROCROP) and Fundación de la Asociación Española Contra el Cáncer (AECC). M.F.S. is supported by a Miguel Servet contract from Instituto de Salud Carlos III, Fondo de Investigación Sanitaria (Spain). The results shown here are in part based on data generated by the TCGA Research Network (<https://www.cancer.gov/tcga>). Writing and editorial assistance was provided by B. L. Phillips of Chrysalis Medical Communications, funded by Bristol-Myers Squibb.

## Author contributions

I.M. conceptually designed and supervised the study, performed the data analysis, wrote the manuscript and critically revised the manuscript. K.A.S. conceptually designed and supervised the study, performed data acquisition, analysis or interpretation, wrote the manuscript and critically revised the manuscript. M.C. performed the data acquisition, analysis, or interpretation, conceptually designed the study, served as Bristol-Myers Squibb lead in managing internal Bristol-Myers Squibb efforts across multiple functional groups to assemble data for analysis and figure generation and critically revised the manuscript. M.F.S. conceptually designed and supervised the study, wrote the manuscript and critically revised the manuscript. T.P.R. conceptually designed the study and critically revised the manuscript. P.P. contributed to the data planning, analysis and figure designs for Figs. 1, 2a, Extended Data Figs. 1, 3 and 7. J.G. analyzed TCGA data used in this work and reviewed the TCGA data analysis section of the manuscript. M.Z. performed data acquisition, analysis or interpretation, including statistical analyses, and critically revised the manuscript. A.M.W., S.-P.H., T.C., Y.F., Q.W. and H.Z. performed

the data acquisition, analysis or interpretation and critically revised the manuscript. D.P., D.L. and J.L.P.-G. conceptually designed the study, wrote the manuscript, critically revised the manuscript and performed the data acquisition, analysis or interpretation. T.B. performed the digital pathology image analysis of immunostained histology slides. V.B. performed the computational image analysis of commercial samples stained with CD15 (neutrophil marker) and IL-8 to demonstrate the positive correlation across multiple indications and interpreted the data, which provided additional supporting evidence for the overall hypothesis. V.N. measured levels of IL-8 protein and neutrophil markers in NSCLC and melanoma tumor tissues and analyzed their relationship. N.G. performed the QIF data acquisition and analyses and contributed to the manuscript figures. All authors contributed to and approved the work presented in this study.

## Competing interests

I.M. reports receiving commercial research grants from Bristol-Myers Squibb, Bioncotech, Alligator, AstraZeneca and Roche; has received speakers bureau honoraria from MSD; and is a consultant/advisory board member for Bristol-Myers Squibb, Roche, Genmab, F-Star, Bioncotech, Bayer, Numab, Alligator, Boehringer Ingelheim and AstraZeneca. K.A.S. reports receiving research funding from Genoptix/Navigate (Novartis), Vasculox/Tioma, Tesaro, Moderna Therapeutics, Takeda, Surface Oncology, Pierre-Fabre Research Institute, Merck, Bristol-Myers Squibb, AstraZeneca and Eli Lilly; has received consultant/advisory board fees from Celgene, Moderna Therapeutics, Shattuck Labs, Pierre-Fabre, AbbVie, AstraZeneca, EMD Serono, Ono Pharmaceuticals, Clinica Alemana de Santiago, Dynamo Therapeutics, Torque Therapeutics, Agenus and Takeda; and has received speaker honoraria and/or travel support for meetings from Takeda, Merck, Bristol-Myers Squibb, Fluidigm, Peerview, Biotrac, Cambridge Healthtech Institute, Shattuck Labs and Genentech. J.L.P.-G. reports grants, personal fees and nonfinancial support from Roche, Bristol-Myers Squibb and MSD; and reports grants and personal fees from Ipsen and Eisai, and grants from Incyte and Janssen. M.C., M.Z., S.-P.H., T.C. and Y.F. have a patent ('Combination Therapy with Anti-IL-8 Antibodies and Anti-PD-1 Antibodies for Treating Cancer', publication number WO 2019140150). T.P.R. is a co-inventor in a provisional patent application (application number 62/650047) regarding the use of anti-IL-8 and anti-PD1 for the treatment of cancer. M.C., M.Z., T.C., Y.F., S.-P.H., A.M.W., V.B., D.P., T.B., D.L., T.P.R., P.P., J.G. and H.Z. are current or former employees of Bristol-Myers Squibb, which is developing anti-IL-8 (NCT03400332). T.P.R., A.M.W., D.L. and S.-P.H. own stock in Bristol-Myers Squibb. None of the remaining authors have relevant conflicts of interest to report.

## Additional information

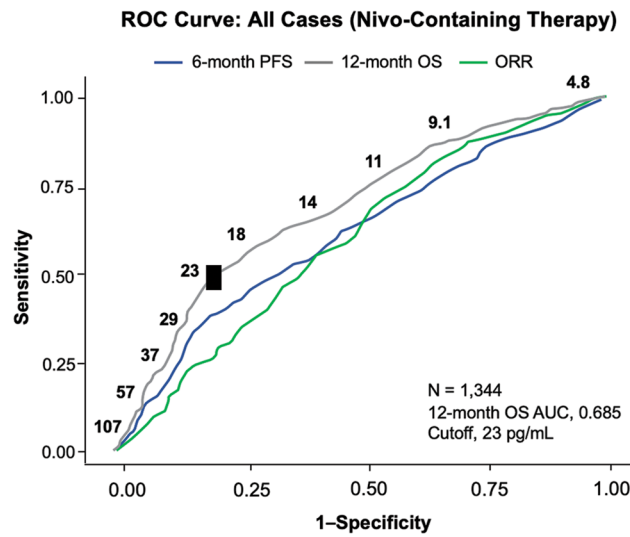
**Extended data** is available for this paper at <https://doi.org/10.1038/s41591-020-0856-x>.

**Supplementary information** is available for this paper at <https://doi.org/10.1038/s41591-020-0856-x>.

**Correspondence and requests for materials** should be addressed to K.A.S. or I.M.

**Peer review information** Saheli Sadanand was the primary editor on this article and managed its editorial process and peer review in collaboration with the rest of the editorial team.

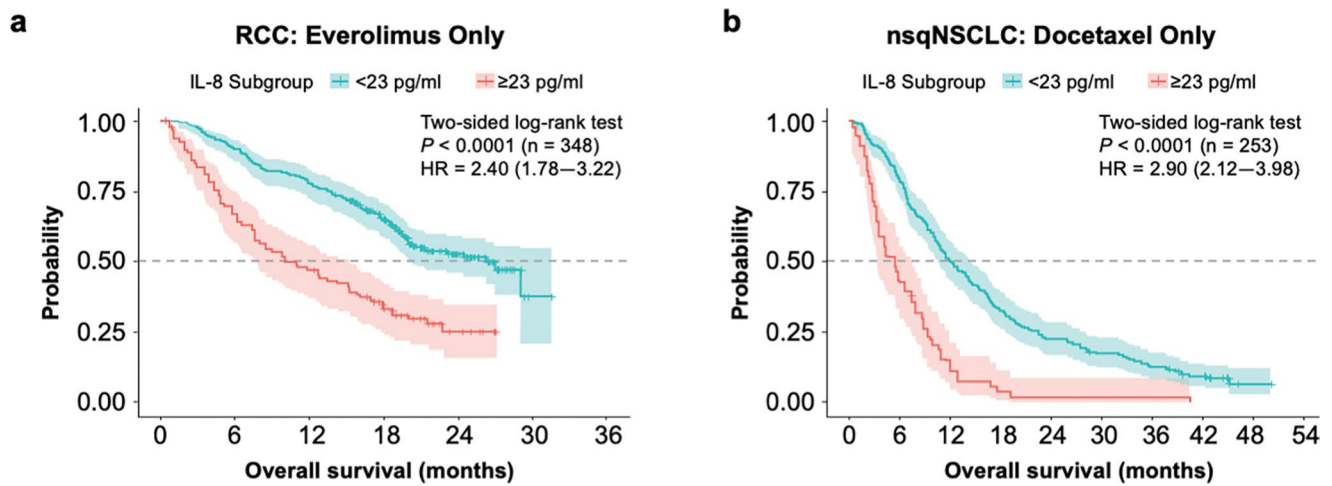
**Reprints and permissions information** is available at [www.nature.com/reprints](http://www.nature.com/reprints).



**Extended Data Fig. 1 | Statistical identification of a baseline serum IL-8 cutoff below which patients were more likely to benefit from Nivo-based therapy.** ROC curve analyses were used to assess ORR, 6-month PFS, and 12-month OS. OS AUC (12-month) is indicated and identifies  $\geq 23$  pg/ml as a cutoff. All cases with nivolumab-containing therapies were analyzed. AUC, area under the curve; Nivo, nivolumab; ORR, objective response rate; OS, overall survival; PFS, progression-free survival; ROC, receiver operator characteristic.

| Study         | Tumor type | Treatment              | n   | Patients with IL-8 $\geq 23$ pg/ml (%) | PFS hazard ratio (95% CI) | OS hazard ratio (95% CI) |
|---------------|------------|------------------------|-----|--|---------------------------|--------------------------|
| CheckMate 067 | Mel        | Nivolumab              | 292 | 28.4                                   | 1.73<br>(1.26–2.38)       | 2.58<br>(1.82–3.66)      |
| CheckMate 067 | Mel        | Ipilimumab             | 298 | 27.1                                   | 1.41<br>(1.06–1.88)       | 2.06<br>(1.52–2.80)      |
| CheckMate 067 | Mel        | Nivolumab + ipilimumab | 297 | 28.3                                   | 2.13<br>(1.54–2.96)       | 3.06<br>(2.13–4.41)      |
| CheckMate 025 | RCC        | Nivolumab              | 392 | 31.4                                   | 1.36<br>(1.07–1.72)       | 2.56<br>(1.89–3.45)      |
| CheckMate 017 | sqNSCLC    | Nivolumab              | 108 | 34.3                                   | 1.28<br>(0.81–2.00)       | 1.84<br>(1.19–2.83)      |
| CheckMate 057 | nsqNSCLC   | Nivolumab              | 255 | 30.6                                   | 1.60<br>(1.19–2.15)       | 1.90<br>(1.42–2.53)      |

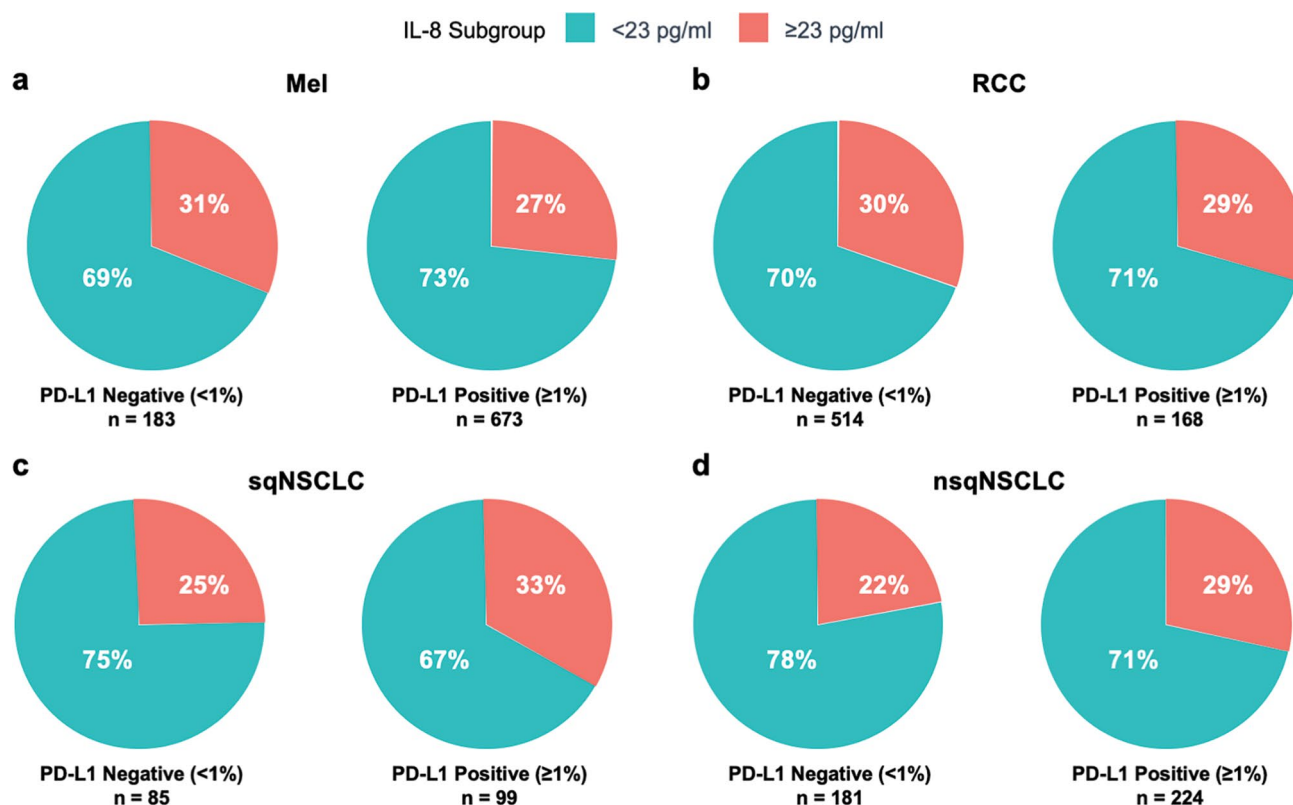
**Extended Data Fig. 2 | Association between elevated IL-8 and survival across treatments and tumor types.** Percentage of patients with baseline serum IL-8 levels  $\geq 23$  pg/ml across Mel (CheckMate 067: nivolumab, n = 292; ipilimumab, n = 298; nivolumab plus ipilimumab, n = 297), RCC (CheckMate 025, n = 392), sqNSCLC (CheckMate 017, n = 108), and nsqNSCLC (CheckMate 057, n = 255) with nivolumab monotherapy, ipilimumab monotherapy, or nivolumab plus ipilimumab combination therapy, as indicated. PFS and OS hazard ratios (IL-8  $\geq 23$  pg/ml versus IL-8 < 23 pg/ml) are also presented (95% CI). HR, hazard ratio; IL, interleukin; Mel, melanoma; nsqNSCLC, nonsquamous non-small cell lung cancer; OS, overall survival; PFS, progression-free survival; RCC, renal cell carcinoma; sqNSCLC, squamous NSCLC.



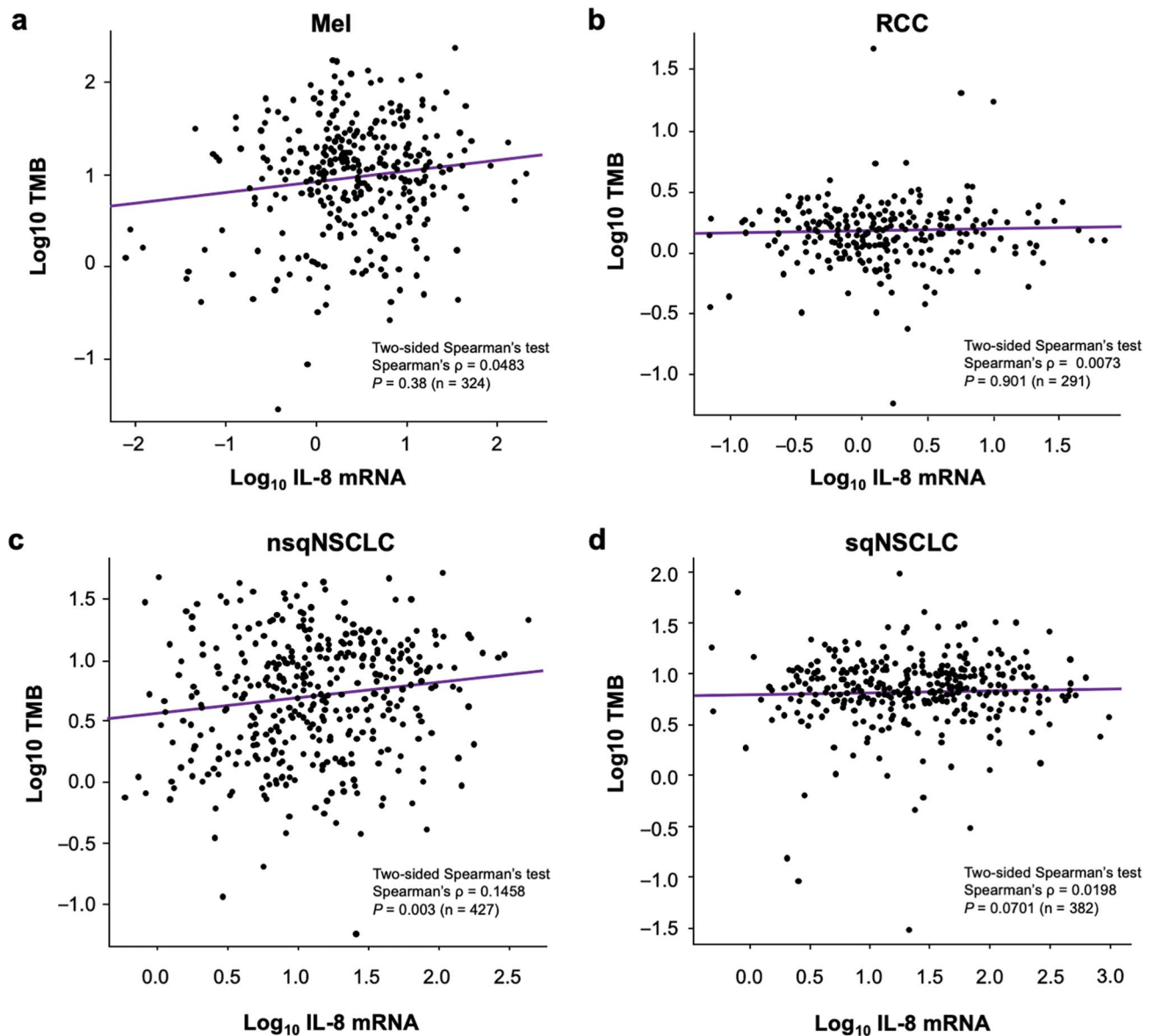
**Extended Data Fig. 3 | Association between elevated IL-8 level and reduced survival was also seen in the non-immunotherapy trial arms.** The specific study, 2-sided log-rank test  $P$  values for the survival analysis, the number of independent patients with available IL-8 and OS data ( $n$ ), and the OS HR (based on Cox proportional hazard model) between IL-8 subgroups ( $\geq 23$  pg/ml versus  $< 23$  pg/ml) are indicated within each chart. **a**, Probability of OS with  $< 23$  pg/ml or  $\geq 23$  pg/ml IL-8 levels in patients with RCC treated with everolimus from CheckMate 025 ( $n = 348$ ). **b**, Probability of OS with  $< 23$  pg/ml or  $\geq 23$  pg/ml IL-8 levels in patients with nsqNSCLC treated with docetaxel from CheckMate 057 ( $n = 253$ ). HR, hazard ratio; IL, interleukin; nsqNSCLC, nonsquamous non-small cell lung cancer; OS, overall survival; RCC, renal cell carcinoma.

| Study         | Tumor type | Treatment              | IL-8 subgroup | <i>n</i> | Number of responders <sup>a</sup> | ORR   |
|---------------|------------|------------------------|---------------|----------|-----------------------------------|-------|
| CheckMate 067 | Mel        | Nivolumab              | <23 pg/ml     | 209      | 98                                | 0.469 |
|               |            |                        | ≥23 pg/ml     | 83       | 24                                | 0.289 |
|               |            | Nivolumab + ipilimumab | <23 pg/ml     | 213      | 124                               | 0.582 |
|               |            |                        | ≥23 pg/ml     | 84       | 29                                | 0.345 |
|               |            | Ipilimumab             | <23 pg/ml     | 217      | 37                                | 0.171 |
|               |            |                        | ≥23 pg/ml     | 81       | 8                                 | 0.099 |
| CheckMate 025 | RCC        | Nivolumab              | <23 pg/ml     | 269      | 75                                | 0.279 |
|               |            |                        | ≥23 pg/ml     | 123      | 24                                | 0.195 |
|               |            | Everolimus             | <23 pg/ml     | 241      | 13                                | 0.054 |
|               |            |                        | ≥23 pg/ml     | 107      | 6                                 | 0.056 |
| CheckMate 017 | sqNSCLC    | Nivolumab              | <23 pg/ml     | 71       | 20                                | 0.282 |
|               |            |                        | ≥23 pg/ml     | 37       | 3                                 | 0.081 |
| CheckMate 057 | nsqNSCLC   | Nivolumab              | <23 pg/ml     | 177      | 42                                | 0.237 |
|               |            |                        | ≥23 pg/ml     | 78       | 8                                 | 0.103 |
|               |            | Docetaxel              | <23 pg/ml     | 197      | 33                                | 0.168 |
|               |            |                        | ≥23 pg/ml     | 56       | 2                                 | 0.036 |

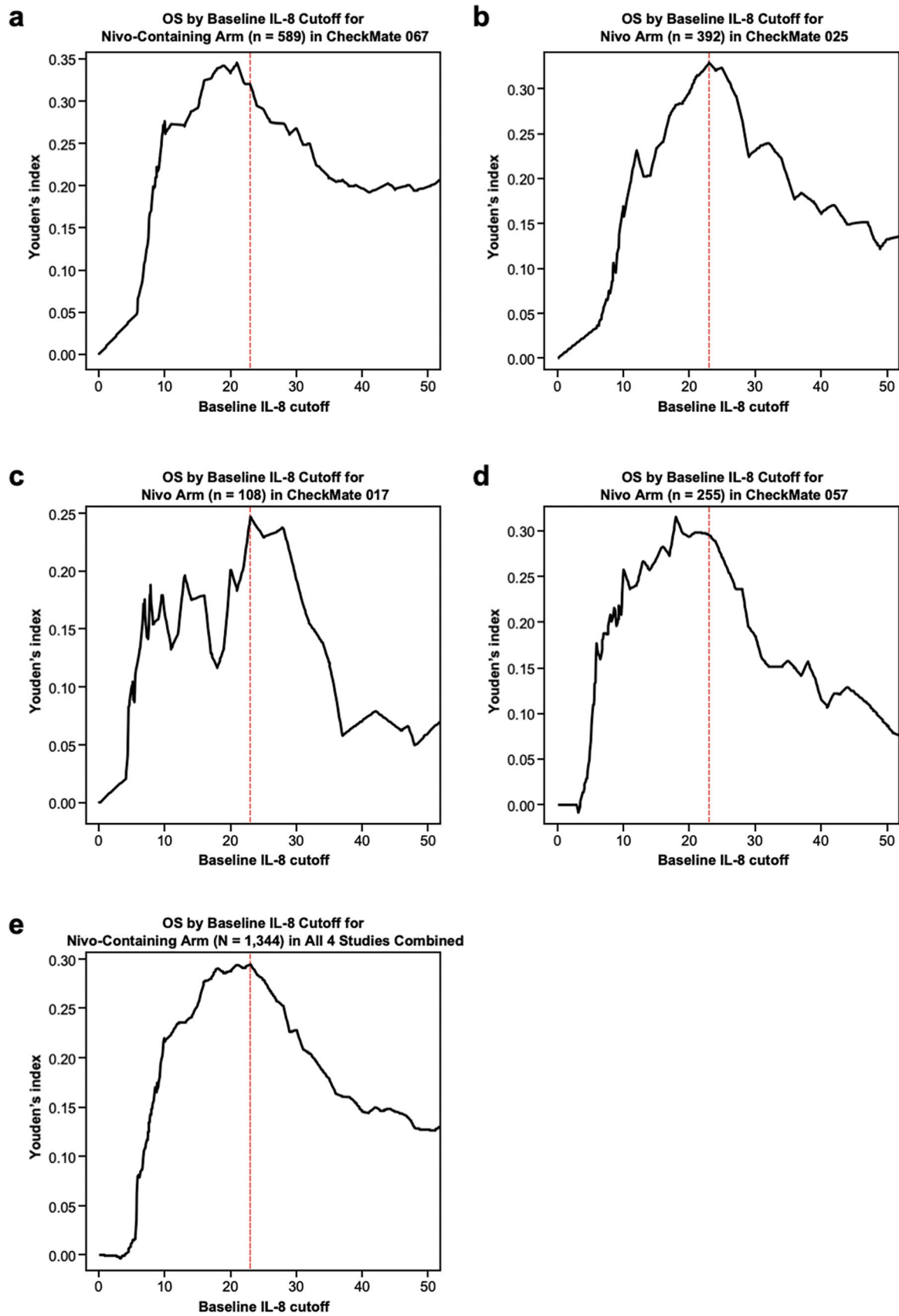
**Extended Data Fig. 4 | ORR by IL-8 subgroup across trials and treatment arms.** ORR vs baseline serum IL-8 levels <23 pg/ml or ≥23 pg/ml across treatment arms in CheckMate 067 (Mel), CheckMate 025 (RCC), CheckMate 017 (sqNSCLC), and CheckMate 057 (nsqNSCLC). IL, interleukin; Mel, melanoma; nsqNSCLC, nonsquamous non-small cell lung cancer; ORR, objective response rate; RCC, renal cell carcinoma; sqNSCLC, squamous NSCLC. <sup>a</sup>Patients with complete response or partial response per RECIST v1.1.



**Extended Data Fig. 5 | Percentage of patients in each IL-8 subgroup by PD-L1 status (negative or positive) across cohorts.** Percentage of patients with baseline serum IL-8 levels <23 pg/ml or ≥23 pg/ml by PD-L1 status (negative [ $<1\%$ ] or positive [ $\geq 1\%$ ]) in Mel (CheckMate 067 [PD-L1  $<1\%$ ,  $n=183$ ; PD-L1  $\geq 1\%$ ,  $n=673$ ;  $P=0.296$ ]) (a), RCC (CheckMate 025 [PD-L1  $<1\%$ ,  $n=514$ ; PD-L1  $\geq 1\%$ ,  $n=168$ ;  $P=0.884$ ]) (b), sqNSCLC (CheckMate 017 [PD-L1  $<1\%$ ,  $n=85$ ; PD-L1  $\geq 1\%$ ,  $n=99$ ;  $P=0.263$ ]) (c), and nsqNSCLC (CheckMate 057 [PD-L1  $<1\%$ ,  $n=181$ ; PD-L1  $\geq 1\%$ ,  $n=224$ ;  $P=0.171$ ]) (d). IL, interleukin; Mel, melanoma; nsqNSCLC, nonsquamous non-small cell lung cancer; PD-L1, programmed death-ligand 1; RCC, renal cell carcinoma; sqNSCLC, squamous NSCLC;  $P$ ,  $p$ -value for chi-squared test of independence between IL-8 subgroup ( $\geq 23$  pg/ml vs  $< 23$  pg/ml) and PD-L1 status ( $\geq 1\%$  vs  $< 1\%$ ).



**Extended Data Fig. 6 | Association between IL-8 expression and TMB in human malignancies.** Association between IL-8 mRNA expression and TMB in human Mel (**a**,  $n = 324$ ), RCC (**b**,  $n = 291$ ), nsqNSCLC (**c**,  $n = 427$ ), and sqNSCLC (**d**,  $n = 382$ ) from TCGA cohort. The levels of IL-8 transcripts are presented as  $\log_{10}$  transformed FPKM units. TMB level was determined as previously reported, including both nonsynonymous and synonymous variants. Dots represent individual samples. Linear regression lines are indicated by purple lines within each chart. IL, interleukin; FPKM, kilobase per million mapped reads; Mel, melanoma; nsqNSCLC, nonsquamous non-small cell lung cancer; RCC, renal cell carcinoma; sqNSCLC, squamous NSCLC; TMB, tumor mutational burden.

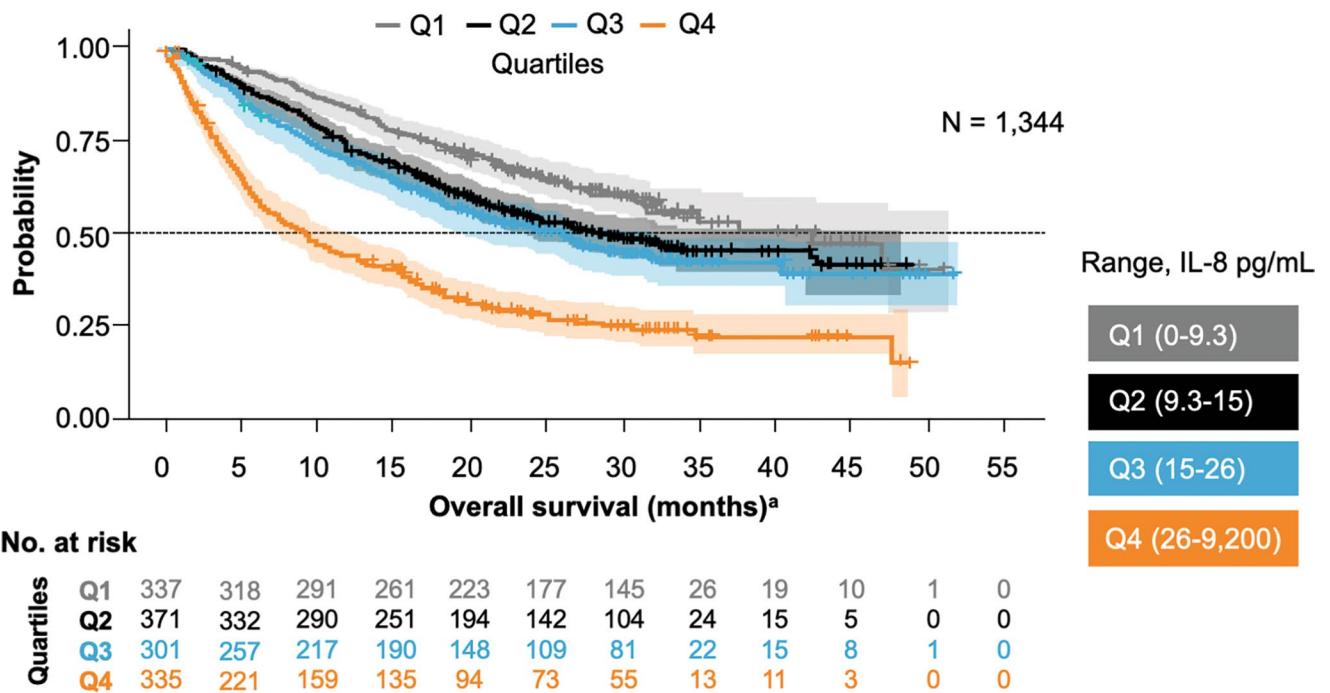


**Extended Data Fig. 7 | Youden's index by baseline IL-8 cutoff (in pg/ml) from OS ROC curve analyses.** Determination of optimal IL-8 cutoff value for the Nivo-containing arm of CheckMate 067 (n = 589) (**a**), nivolumab arm of CheckMate 025 (n = 392) (**b**), nivolumab arm of CheckMate 017 (n = 108) (**c**), nivolumab arm of CheckMate 057 (n = 255) (**d**), and all studies pooled (N = 1,344) (**e**). Red dotted lines indicate 23 pg/ml. IL, interleukin; Nivo, nivolumab; OS, overall survival; ROC, receiver operating characteristic.

| Nivolumab trial                           | Trial description   |
|---|---|
| <b>Mel (<i>n</i> = 589<sup>a</sup>)</b>   |   |
| CheckMate 067<br>(NCT01844505)            | CheckMate 067 is a phase 3, randomized, double-blind study of nivolumab monotherapy or nivolumab combined with ipilimumab versus ipilimumab monotherapy in adult patients with previously untreated, unresectable, or metastatic melanoma. In experimental arm A, patients received nivolumab at a dose of 3 mg/kg intravenously every 2 weeks matching with ipilimumab 0 mg/kg solution intravenously on weeks 1, 4, and placebo matching with nivolumab on weeks 4 for cycles 1 and 2. In experimental arm B, patients received nivolumab 1 mg/kg intravenously combined with ipilimumab 3 mg/kg intravenously every 3 weeks for 4 doses then nivolumab 3 mg/kg intravenously every 2 weeks plus placebo matching with nivolumab on weeks 3 and 5 for cycles 1 and 2. Primary endpoints include progression-free survival and overall survival. |
| <b>NSCLC (<i>n</i> = 363<sup>a</sup>)</b> |   |
| CheckMate 017<br>(NCT01642004)            | CheckMate 017 is a randomized, open-label, phase 3 study that evaluated the efficacy and safety of nivolumab, as compared with docetaxel, in patients with sqNSCLC after failure of platinum-based chemotherapy. Patients received nivolumab at a dose of 3 mg/kg every 2 weeks or docetaxel at a dose of 75 mg per square meter of body-surface area every 3 weeks. The primary endpoints include overall survival, overall survival rate, and safety.   |
| CheckMate 057<br>(NCT01673867)            | CheckMate 057 is a randomized, open-label, phase 3 study that assigned patients with nsqNSCLC that had progressed during or after platinum-based doublet chemotherapy to receive nivolumab at a dose of 3 mg/kg every 2 weeks or docetaxel at a dose of 75 mg per square meter of body-surface area every 3 weeks. The primary endpoint is overall survival.  |
| <b>RCC (<i>n</i> = 392<sup>a</sup>)</b>   |   |
| CheckMate 025<br>(NCT01668784)            | CheckMate 025 is a randomized, open-label, phase 3 study comparing nivolumab with everolimus in patients with advanced or metastatic cell-cell RCC who had received previous anti-angiogenic treatment. Patients received nivolumab at a dose of 3 mg/kg intravenously every 2 weeks or everolimus at a dose of 10 mg tablets by mouth daily. The primary endpoint is overall survival.   |

**Extended Data Fig. 8 | Peripheral blood and tumor samples from 1,344 patients treated with nivolumab or nivolumab plus ipilimumab in 4 phase 3 clinical trials included in the analyses.** Summary of 4 phase 3 clinical trials (CheckMate 067, CheckMate 017, CheckMate 057, CheckMate 025, *N* = 1,344 patients). IL, interleukin; Mel, melanoma; nsqNSCLC, nonsquamous non-small cell lung cancer; RCC, renal cell carcinoma; sqNSCLC, squamous NSCLC.

<sup>a</sup>Includes patients who were treated with nivolumab or nivolumab + ipilimumab and had nonmissing serum IL-8 levels.



**Extended Data Fig. 9 | Kaplan-Meier analyses to assess overall survival stratified by baseline serum IL-8 levels.** Analysis of pooled data from 1,344 patients receiving nivolumab-based therapy in 4 phase 3 trials—including patients with melanoma, renal cell carcinoma, squamous non-small cell lung cancer, and nonsquamous non-small cell lung cancer—confirmed that elevated baseline serum IL-8 levels were associated with overall survival. This association was significant after adjustment for baseline tumor burden and tumor programmed death-ligand 1 expression ( $P < 0.001$ ). <sup>a</sup>OS data from patients in CheckMate trials –017, –057, –067, –025. IL, interleukin.

## Reporting Summary

Nature Research wishes to improve the reproducibility of the work that we publish. This form provides structure for consistency and transparency in reporting. For further information on Nature Research policies, see [Authors & Referees](#) and the [Editorial Policy Checklist](#).

### Statistics

For all statistical analyses, confirm that the following items are present in the figure legend, table legend, main text, or Methods section.

n/a Confirmed

- The exact sample size ( $n$ ) for each experimental group/condition, given as a discrete number and unit of measurement
- A statement on whether measurements were taken from distinct samples or whether the same sample was measured repeatedly
- The statistical test(s) used AND whether they are one- or two-sided  
*Only common tests should be described solely by name; describe more complex techniques in the Methods section.*
- A description of all covariates tested
- A description of any assumptions or corrections, such as tests of normality and adjustment for multiple comparisons
- A full description of the statistical parameters including central tendency (e.g. means) or other basic estimates (e.g. regression coefficient) AND variation (e.g. standard deviation) or associated estimates of uncertainty (e.g. confidence intervals)
- For null hypothesis testing, the test statistic (e.g.  $F$ ,  $t$ ,  $r$ ) with confidence intervals, effect sizes, degrees of freedom and  $P$  value noted  
*Give  $P$  values as exact values whenever suitable.*
- For Bayesian analysis, information on the choice of priors and Markov chain Monte Carlo settings
- For hierarchical and complex designs, identification of the appropriate level for tests and full reporting of outcomes
- Estimates of effect sizes (e.g. Cohen's  $d$ , Pearson's  $r$ ), indicating how they were calculated

*Our web collection on [statistics for biologists](#) contains articles on many of the points above.*

### Software and code

Policy information about [availability of computer code](#)

Data collection

Data were from BMS clinical trial database.

Data analysis

SAS v9.4 and R version 3.6 were used for data analyses.

For manuscripts utilizing custom algorithms or software that are central to the research but not yet described in published literature, software must be made available to editors/reviewers. We strongly encourage code deposition in a community repository (e.g. GitHub). See the Nature Research [guidelines for submitting code & software](#) for further information.

### Data

Policy information about [availability of data](#)

All manuscripts must include a [data availability statement](#). This statement should provide the following information, where applicable:

- Accession codes, unique identifiers, or web links for publicly available datasets
- A list of figures that have associated raw data
- A description of any restrictions on data availability

K.A.S.'s laboratory designed, conducted, analyzed, and interpreted data presented in Fig. 2b-j and Extended Data 6 (Yale Human Investigation Committee protocols 9505008219 and 1608018220). Bristol-Myers Squibb funded the studies CheckMate 067 (NCT01844505), CheckMate 017 (NCT01642004), CheckMate 057 (NCT01673867), CheckMate 025 (NCT01668784), CheckMate 038 (NCT01621490), and CheckMate 064 (NCT01783938) and participated in the design, conduct, analyses, and interpretation of these studies and related data (Fig. 1, Fig. 2a, Extended Data 1, Extended Data 2, Extended Data 3, Extended Data 5, Extended Data 7, Extended Data 8, and Extended Data 9). Source data for Fig. 1, 2, and Extended Data 4 are presented in the Supplementary Dataset. Bristol-Myers Squibb's policy on data sharing may be found at <https://www.bms.com/researchers-and-partners/independent-research/data-sharing-request-process.html>.

## Field-specific reporting

Please select the one below that is the best fit for your research. If you are not sure, read the appropriate sections before making your selection.

Life sciences       Behavioural & social sciences       Ecological, evolutionary & environmental sciences

For a reference copy of the document with all sections, see [nature.com/documents/nr-reporting-summary-flat.pdf](https://www.nature.com/documents/nr-reporting-summary-flat.pdf)

## Life sciences study design

All studies must disclose on these points even when the disclosure is negative.

|                 |   |
|-----------------|---|
| Sample size     | Patients who were treated with nivolumab or nivolumab + ipilimumab and had nonmissing baseline serum IL-8 levels from 4 phase 3 clinical trials were included for analyses. Sample sizes for each of the 4 studies (CheckMate 067, -017, -057, -025) are justified in the sample size justification section of the respective protocols.  |
| Data exclusions | had missing baseline IL-8 levels could not included in the exploratory analysis. Additionally, for exploratory analyses of the association between PD-L1 and IL-8 levels, patients with either missing PD-L1 or IL-8 levels were not included. Assessment of baseline IL-8 levels was not a criteria of the clinical trials used for the retrospective analysis.  |
| Replication     | IL-8 data from the 4 phase 3 clinical trials were validated. R or SAS programs were archived to ensure reproducibility. Source data sets are also disclosed to ensure transparency and reproducibility. There are no multiplicity adjustments made for all statistical testing. The data presented in Figure 2 using multiplexed immunofluorescence analysis represents multiple tumor specimens from each tumor cohort (variable number per tumor between 99-307) analyzed in one experimental run. This is typical for human tumor tissue studies where the same tissue area/ exact cells cannot be analyzed more than once and replicates may introduce variations due to tissue heterogeneity or spatial variation. |
| Randomization   | All 4 phase 3 clinical trials were randomized.  |
| Blinding        | CheckMate 067 is a double-blind, randomized, phase 3 study. CheckMate 017, -057, and -025 are all open-label, randomized, phase 3 studies   |

## Reporting for specific materials, systems and methods

We require information from authors about some types of materials, experimental systems and methods used in many studies. Here, indicate whether each material, system or method listed is relevant to your study. If you are not sure if a list item applies to your research, read the appropriate section before selecting a response.

### Materials & experimental systems

| n/a                                 | Involved in the study   |
|-------------------------------------|---|
| <input type="checkbox"/>            | <input checked="" type="checkbox"/> Antibodies                  |
| <input checked="" type="checkbox"/> | <input type="checkbox"/> Eukaryotic cell lines                  |
| <input checked="" type="checkbox"/> | <input type="checkbox"/> Palaeontology                          |
| <input checked="" type="checkbox"/> | <input type="checkbox"/> Animals and other organisms            |
| <input type="checkbox"/>            | <input checked="" type="checkbox"/> Human research participants |
| <input type="checkbox"/>            | <input checked="" type="checkbox"/> Clinical data               |

### Methods

| n/a                                 | Involved in the study                           |
|-------------------------------------|---|
| <input checked="" type="checkbox"/> | <input type="checkbox"/> ChIP-seq               |
| <input checked="" type="checkbox"/> | <input type="checkbox"/> Flow cytometry         |
| <input checked="" type="checkbox"/> | <input type="checkbox"/> MRI-based neuroimaging |

## Antibodies

|                 |  |
|-----------------|--|
| Antibodies used | Pancytokeratin clone AE1/AE3 (1:100 dilution; cat# 53-9003-82; eBioscience), IL-8 clone 807 (1:5,000 dilution; cat#ab18672; Abcam), myeloperoxidase clone E1E71 (1:1,000 dilution; cat#14569; Cell Signaling Technology), and CD15 clone MC480 (1:2,000 dilution; cat#4744S; Cell Signaling Technology)  |
| Validation      | We used a previously reported antibody validation strategy (Biotechniques. 2010, 48:197-209). Specificity was demonstrated by the detection of signal in positive control FFPE cell line preparations and human nontumor tissues. Standardization of each assay was performed testing at least 5 dilution/titer points and determining the highest signal to noise ratio. Reproducibility of the staining was assessed by analyzing control/index tissue microarray samples at different time points and showing a linear regression coefficient >0.8 across runs. The multiplexed immunofluorescence experiments were conducted and analyzed using a previously validated protocol (J Natl Cancer Inst 2015, 107(3). pii: dju435.). Data for assay validation/standardization can be provided upon request. |

## Human research participants

Policy information about [studies involving human research participants](#)

Population characteristics      or selected experiments presented in Figure 2, we analyzed lung cancer, melanoma, and renal cell carcinoma cohorts including

|                            |   |
|----------------------------|---|
| Population characteristics | archive tumor tissue collected at the Yale Pathology suite. Cases were selected solely based on their histopathology diagnosis and tumor tissue availability.   |
| Recruitment                | Samples were collected retrospectively from the Yale Pathology archive and annotated for major clinicopathologic variables through review of pathology reports and clinical records by trained personnel.                             |
| Ethics oversight           | All tissue and clinical information were used after approval from the Yale Human Investigation Committee protocols #9505008219 and #1608018220 (PI: Kurt A. Schalper), which approved the patient consent forms or waiver of consent. |

Note that full information on the approval of the study protocol must also be provided in the manuscript.

## Clinical data

Policy information about [clinical studies](#)

All manuscripts should comply with the ICMJE [guidelines for publication of clinical research](#) and a completed [CONSORT checklist](#) must be included with all submissions.

|                             |   |
|-----------------------------|---|
| Clinical trial registration | NCT01844505; NCT01642004; NCT01673867; NCT01668784  |
| Study protocol              | Studies: CheckMate 067, -017, -057, -025. Information about the specific Human Investigation Committee protocols used in the study is provided in the "Ethics oversight" question above. Yale Human Investigation Committee protocols: #9505008219, #1608018220 |
| Data collection             | Baseline PD-L1 and IL-8 levels, and efficacy data (eg, ORR, OS), were collected per the methods and schedules defined in the study protocols (eg, CheckMate 097, -017, -057, -025).   |
| Outcomes                    | Efficacy outcomes (eg, ORR, OS) were predefined in the study protocols and were assessed based on protocol-defined procedures.  |